

## Supporting Information

### Thermal Atomic Layer Deposition of Er<sub>2</sub>O<sub>3</sub> Films from a Volatile, Thermally Stable Enaminolate Precursor

Navoda Jayakodiarachchi,<sup>a</sup> Rui Liu,<sup>b</sup> Chamod Dharmadasa,<sup>a</sup> Xiaobing Hu,<sup>c</sup> Donald E. Savage,<sup>b</sup> Cassandra L. Ward,<sup>a</sup> Paul G. Evans,<sup>b</sup> and Charles H. Winter\*<sup>a</sup>

<sup>a</sup>Department of Chemistry, Wayne State University, Detroit, Michigan 48202 USA.

<sup>b</sup>Department of Materials Science and Engineering, University of Wisconsin-Madison, Madison, Wisconsin 53706 USA.

<sup>c</sup>Department of Materials Science and Engineering and Atomic and Nanoscale Characterization Experimental Center, Northwestern University, Evanston, Illinois 60208, USA.

#### Corresponding Author

\*E-mail: chw@chem.wayne.edu

### X-ray crystallographic details

The crystal structure of **1** was collected on a Bruker D8 Venture diffractometer with kappa geometry, an Incoatec I $\mu$ S micro-focus X-ray source (Mo K $\alpha$  radiation), and a multilayer mirror for monochromatization. The diffraction intensities were measured using a Bruker Photon III CPAD area detector. Data were acquired at 102 K with an Oxford 800 Cryostream low-temperature apparatus. The data were processed using APEX4 software. The structures were solved by Intrinsic Phasing using ShelXT and refined with ShelXL using Olex2. Hydrogen atoms were placed in calculated positions using a standard riding model and refined isotropically; all other atoms were refined anisotropically. The main refinement parameters are listed in Table S1. The crystal structure data were deposited with the Cambridge Crystallographic Data Centre, with the deposition number 2266444.

**Table S1.** Crystal data and structure refinement for **1**.

Identification code	CHW_CD_ErL13_2
Empirical formula	C <sub>24</sub> H <sub>48</sub> ErN <sub>3</sub> O <sub>3</sub>
Formula weight	593.91
Temperature/K	102.00
Crystal system	monoclinic
Space group	P2 <sub>1</sub> /n
a/Å	9.8012(7)
b/Å	21.6980(15)
c/Å	14.4627(11)
α/°	90
β/°	108.316(3)
γ/°	90
Volume/Å <sup>3</sup>	2919.9(4)
Z	4
ρ <sub>calc</sub> g/cm <sup>3</sup>	1.351
μ/mm <sup>-1</sup>	2.899
F(000)	1220.0
Crystal size/mm <sup>3</sup>	0.12 × 0.1 × 0.08
Radiation	Mo Kα ( $\lambda = 0.71073$ )
2θ range for data collection/°	4.764 to 61.082
Index ranges	-14 ≤ h ≤ 14, -31 ≤ k ≤ 31, -20 ≤ l ≤ 20
Reflections collected	128020
Independent reflections	8917 [R <sub>int</sub> = 0.0456, R <sub>sigma</sub> = 0.0173]
Data/restraints/parameters	8917/0/295
Goodness-of-fit on F <sup>2</sup>	1.033
Final R indexes [I>=2σ (I)]	R <sub>1</sub> = 0.0164, wR <sub>2</sub> = 0.0358
Final R indexes [all data]	R <sub>1</sub> = 0.0190, wR <sub>2</sub> = 0.0366

**Table S2.** Bond Lengths for **1**.

<b>Atom</b>	<b>Atom</b>	<b>Length/Å</b>	<b>Atom</b>	<b>Atom</b>	<b>Length/Å</b>
Er1	O3	2.1447(10)	N2	C9	1.4563(19)
Er1	O2	2.1589(10)	C18	C19	1.5199(19)
Er1	O1	2.1618(10)	C18	C17	1.332(2)
Er1	N3	2.4980(12)	C19	C21	1.524(2)
Er1	N1	2.5649(11)	C19	C20	1.531(2)
Er1	N2	2.5066(12)	C19	C22	1.532(2)
O3	C18	1.3284(17)	C2	C3	1.5194(19)
O2	C10	1.3288(17)	C2	C1	1.3459(19)
O1	C2	1.3347(16)	C3	C6	1.5280(19)
N3	C17	1.4578(18)	C3	C5	1.533(2)
N3	C23	1.477(2)	C3	C4	1.534(2)
N3	C24	1.479(2)	C10	C9	1.342(2)
N1	C8	1.4848(19)	C10	C11	1.522(2)
N1	C7	1.4721(18)	C11	C12	1.531(2)
N1	C1	1.4539(18)	C11	C13	1.523(2)
N2	C15	1.479(2)	C11	C14	1.530(2)
N2	C16	1.4780(19)			

**Table S3.** Bond Angles for **1**.

<b>Atom</b>	<b>Atom</b>	<b>Atom</b>	<b>Angle/°</b>	<b>Atom</b>	<b>Atom</b>	<b>Atom</b>	<b>Angle/°</b>
O3	Er1	O2	109.41(5)	C9	N2	Er1	105.41(8)
O3	Er1	O1	103.88(4)	C9	N2	C15	110.03(13)
O3	Er1	N3	72.16(4)	C9	N2	C16	109.72(12)
O3	Er1	N1	160.45(4)	O3	C18	C19	115.31(13)
O3	Er1	N2	86.65(4)	O3	C18	C17	120.92(13)
O2	Er1	O1	143.00(4)	C17	C18	C19	123.68(13)
O2	Er1	N3	97.67(4)	C18	C19	C21	109.00(11)
O2	Er1	N1	83.52(4)	C18	C19	C20	108.02(12)
O2	Er1	N2	72.01(4)	C18	C19	C22	112.39(13)
O1	Er1	N3	107.64(4)	C21	C19	C20	109.00(13)
O1	Er1	N1	69.33(4)	C21	C19	C22	108.90(12)
O1	Er1	N2	94.68(4)	C20	C19	C22	109.47(13)
N3	Er1	N1	92.05(4)	C18	C17	N3	120.14(13)
N3	Er1	N2	152.12(4)	O1	C2	C3	115.61(12)
N2	Er1	N1	111.76(4)	O1	C2	C1	120.50(13)
C18	O3	Er1	121.47(9)	C1	C2	C3	123.86(12)
C10	O2	Er1	121.25(9)	C2	C3	C6	112.95(11)
C2	O1	Er1	121.80(9)	C2	C3	C5	107.94(12)
C17	N3	Er1	105.28(8)	C2	C3	C4	108.16(12)
C17	N3	C23	108.32(12)	C6	C3	C5	108.69(12)
C17	N3	C24	109.72(12)	C6	C3	C4	109.41(12)
C23	N3	Er1	112.54(9)	C5	C3	C4	109.64(13)
C23	N3	C24	109.87(12)	O2	C10	C9	120.98(13)
C24	N3	Er1	110.97(9)	O2	C10	C11	114.89(13)
C8	N1	Er1	100.63(8)	C9	C10	C11	124.12(13)
C7	N1	Er1	121.83(9)	C2	C1	N1	117.90(12)

C7	N1	C8	107.87(11)		C10	C9	N2	119.99(13)
C1	N1	Er1	104.97(8)		C10	C11	C12	109.11(12)
C1	N1	C8	109.26(11)		C10	C11	C13	108.27(14)
C1	N1	C7	111.40(12)		C10	C11	C14	112.40(14)
C15	N2	Er1	113.40(9)		C13	C11	C12	108.49(15)
C16	N2	Er1	110.38(9)		C13	C11	C14	110.67(17)
C16	N2	C15	107.87(13)		C14	C11	C12	107.83(15)

**Table S4.** Thickness of an Er<sub>2</sub>O<sub>3</sub> film deposited in a nanoscale trench with aspect ratio = 10. The thicknesses were measured at the locations indicated in Fig. S10.

Position      Thickness (nm)

1	11.02
2	10.2
3	15.9
4	10.01
5	14.12
6	11.01
7	13.03
8	10.21
9	10.58

**Figure S1.** ORTEP image of **1** with thermal ellipsoids at the 50% level. Hydrogen atoms were omitted for clarity.

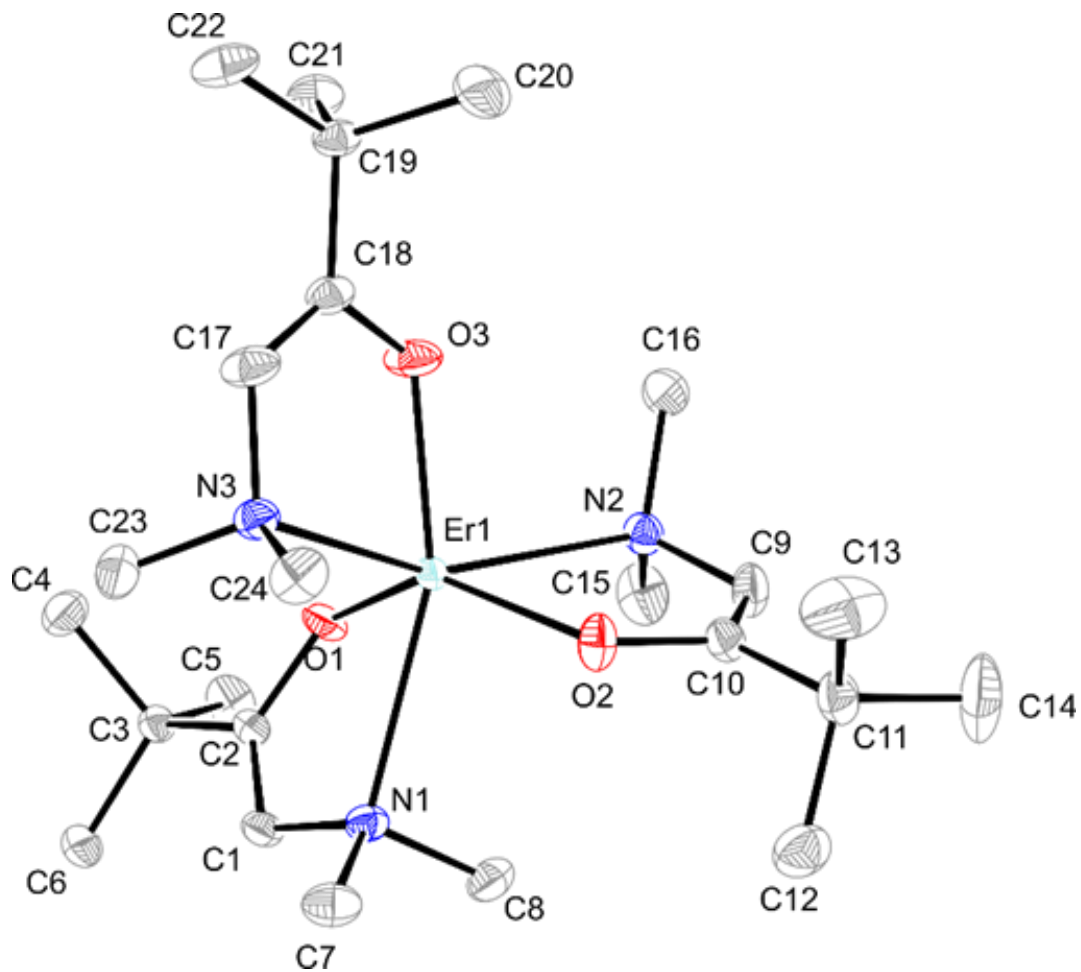


**Figure S2.** The dependence of Er<sub>2</sub>O<sub>3</sub> film thicknesses on the number of ALD cycles on Si(100) substrates at 200 °C substrate temperature.

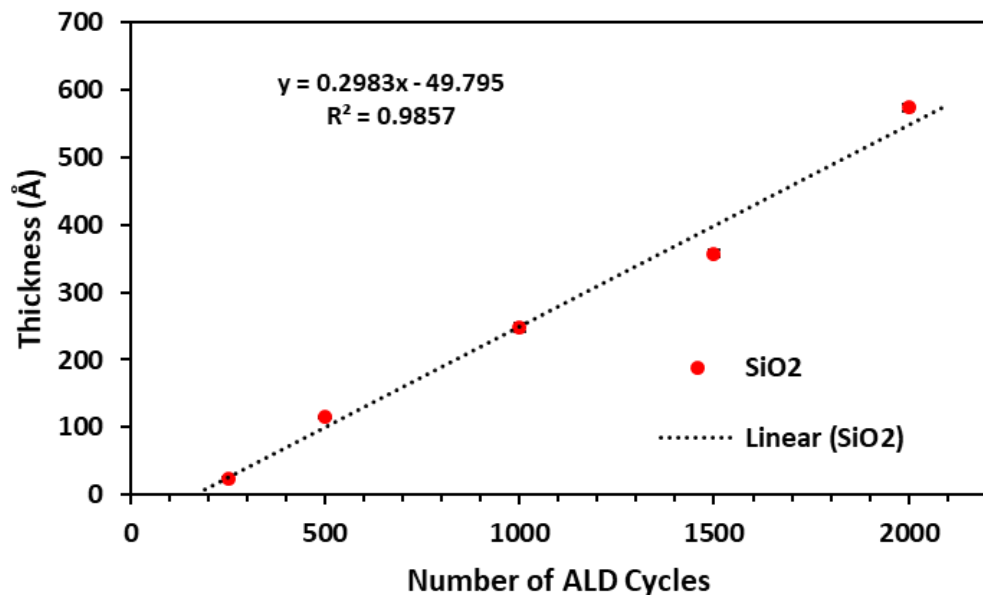


**Figure S3.** XRD patterns of ~20-25 nm as-deposited  $\text{Er}_2\text{O}_3$  thin films deposited at 150, 200, and 250 °C on  $\text{SiO}_2$  substrates with 1000 cycles. The dotted lines represent the reference for cubic  $\text{Er}_2\text{O}_3$  (COD 1010334  $\text{Er}_2\text{O}_3$ ).

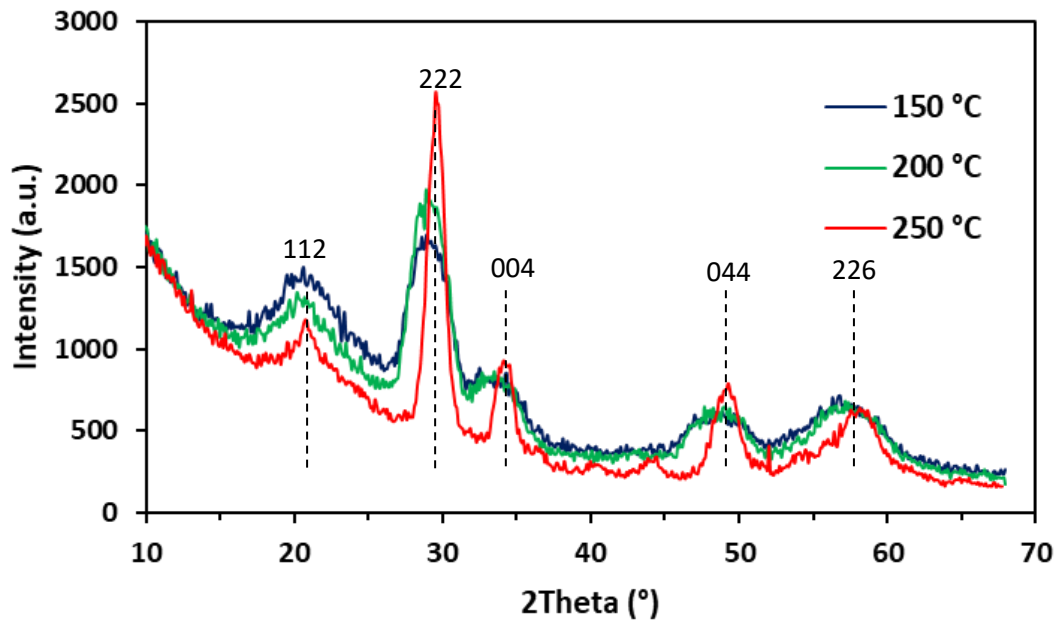


**Figure S4.** XRR fitting curves of 33 nm thick  $\text{Er}_2\text{O}_3$  thin film grown on Si(100) (top, density = 7.3 gm/cm<sup>3</sup>) and  $\text{SiO}_2$  (bottom, density = 7.1 gm/cm<sup>3</sup>) substrates at 200 °C.

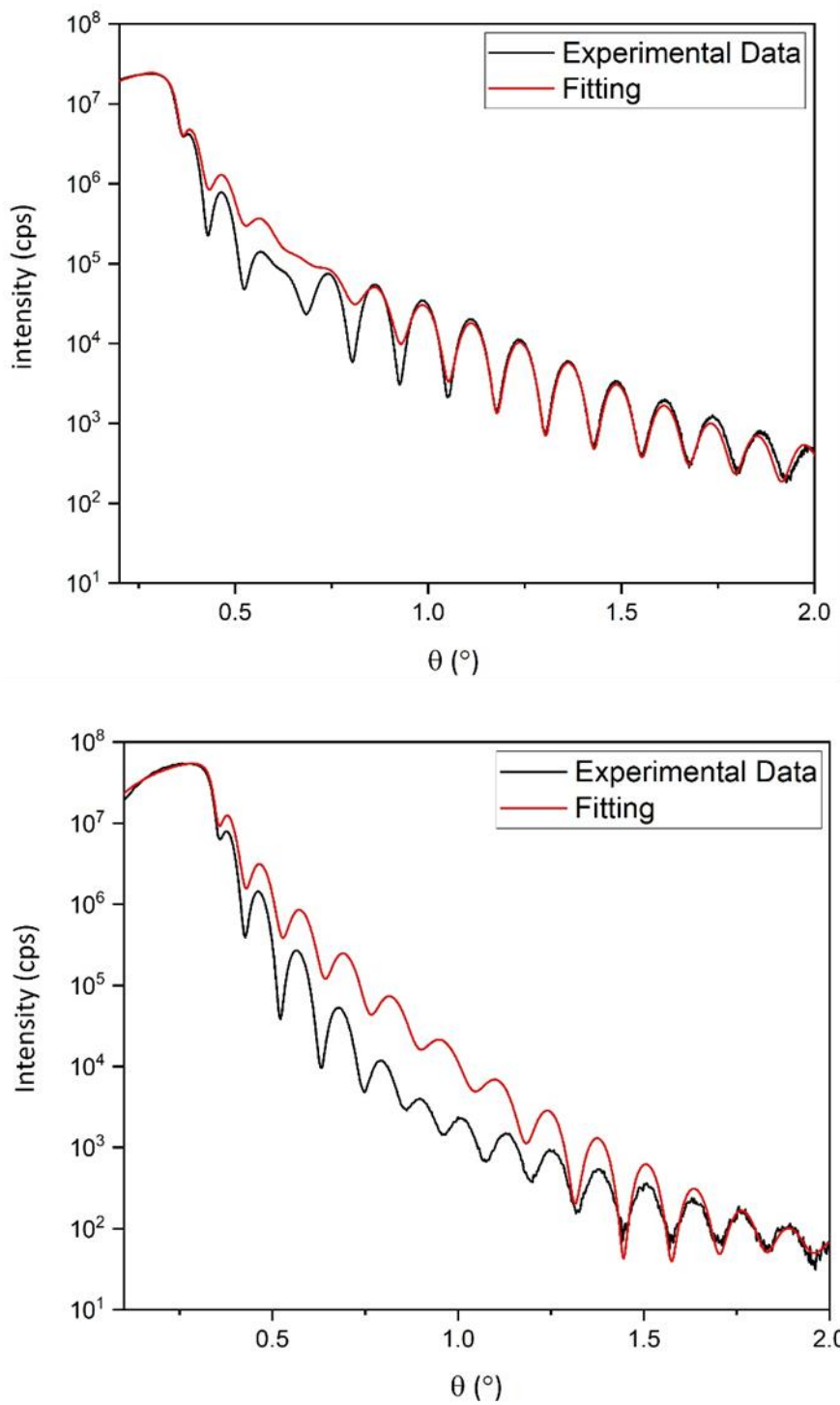


**Figure S5.** Top-down SEM micrographs of Er<sub>2</sub>O<sub>3</sub> thin films deposited with 1500 ALD cycles on Si (left) and SiO<sub>2</sub> (right) substrates at 200 °C.

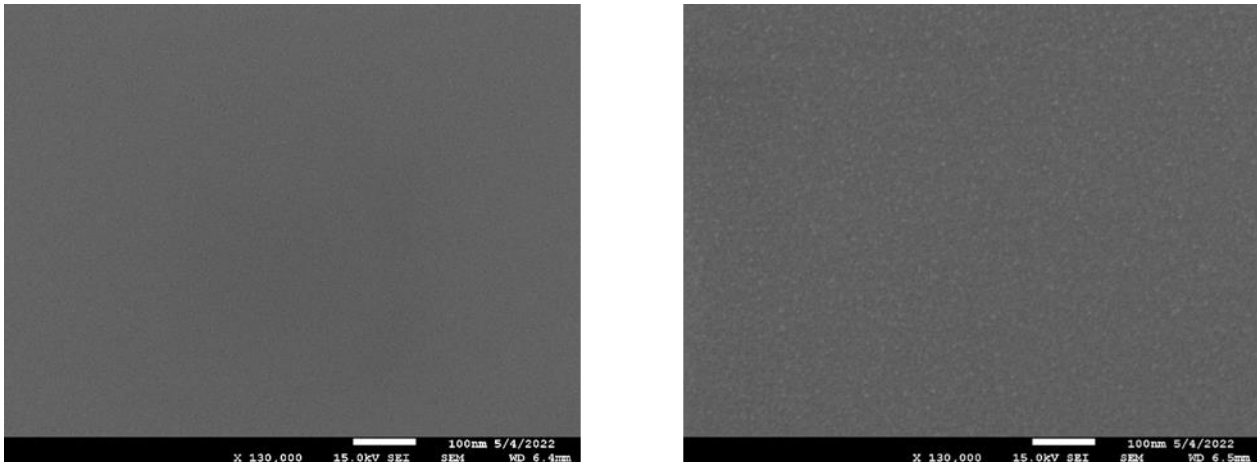


**Figure S6.** Cross-sectional SEM images of  $\text{Er}_2\text{O}_3$  thin films grown on (a) Cu, (b) Ru, (c) TiN, (d) Pt, and (e) W at substrate temperatures of 200 °C with 1500 ALD cycles.

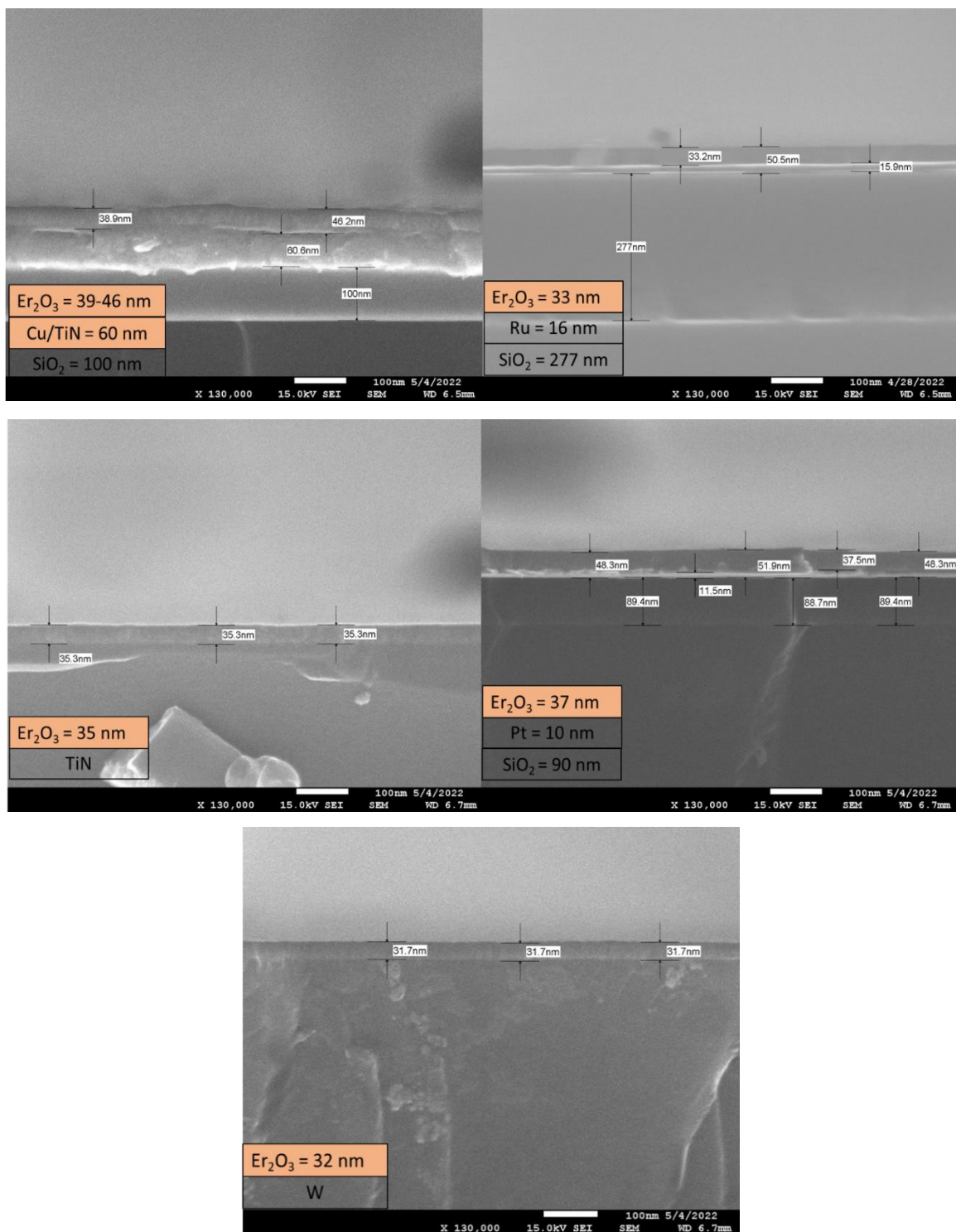


**Figure S7.** GI-XRD patterns of the as-deposited  $\text{Er}_2\text{O}_3$  thin films shown in Fig. S6 grown on Cu, Ru, TiN, Pt, and W at substrate temperatures of 200 °C with 1500 ALD cycles.

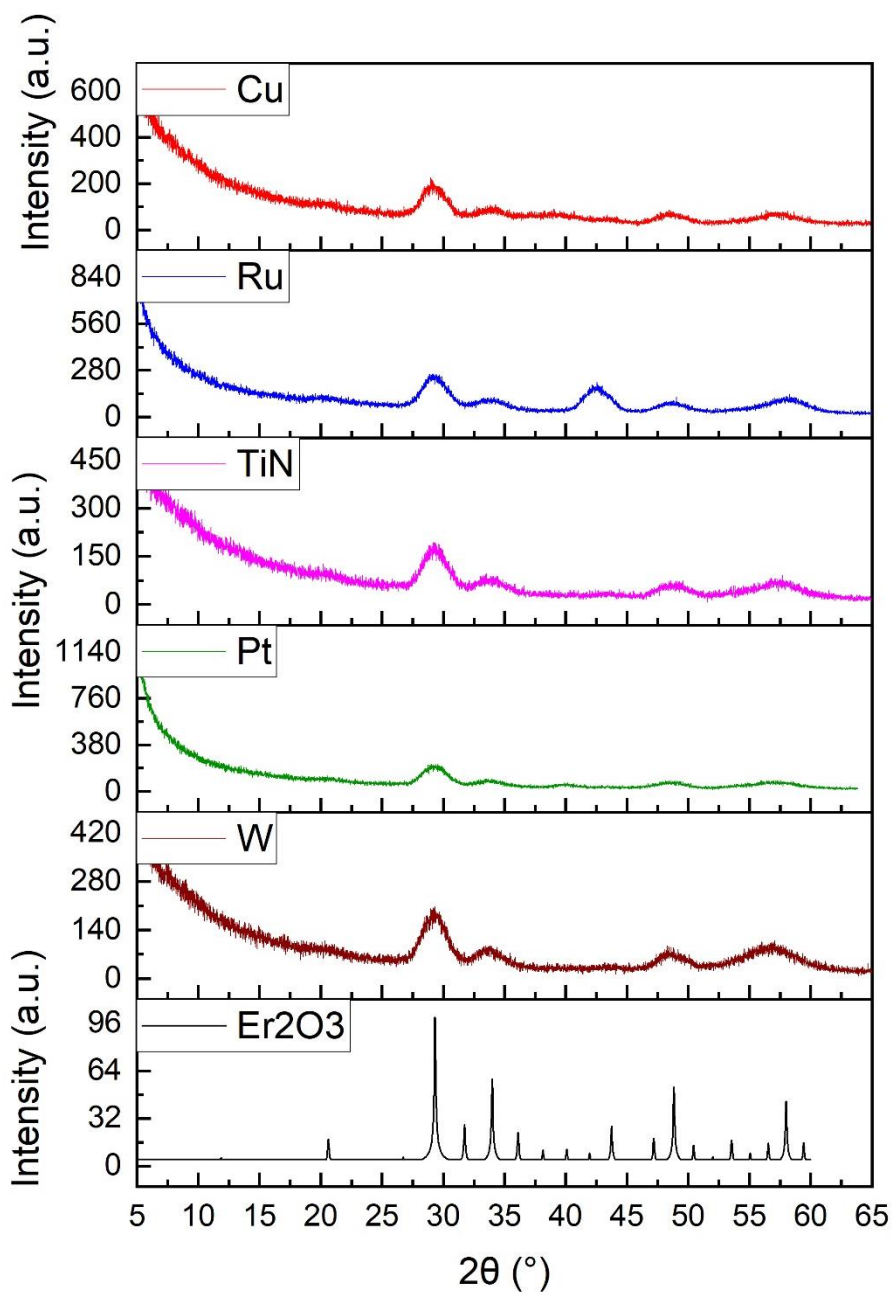


**Figure S8.** GI-XRD patterns of as-deposited  $\text{Er}_2\text{O}_3$  thin films grown on an STO (top) and sapphire (bottom) at substrate temperatures of 200 °C with 1500 ALD cycles.

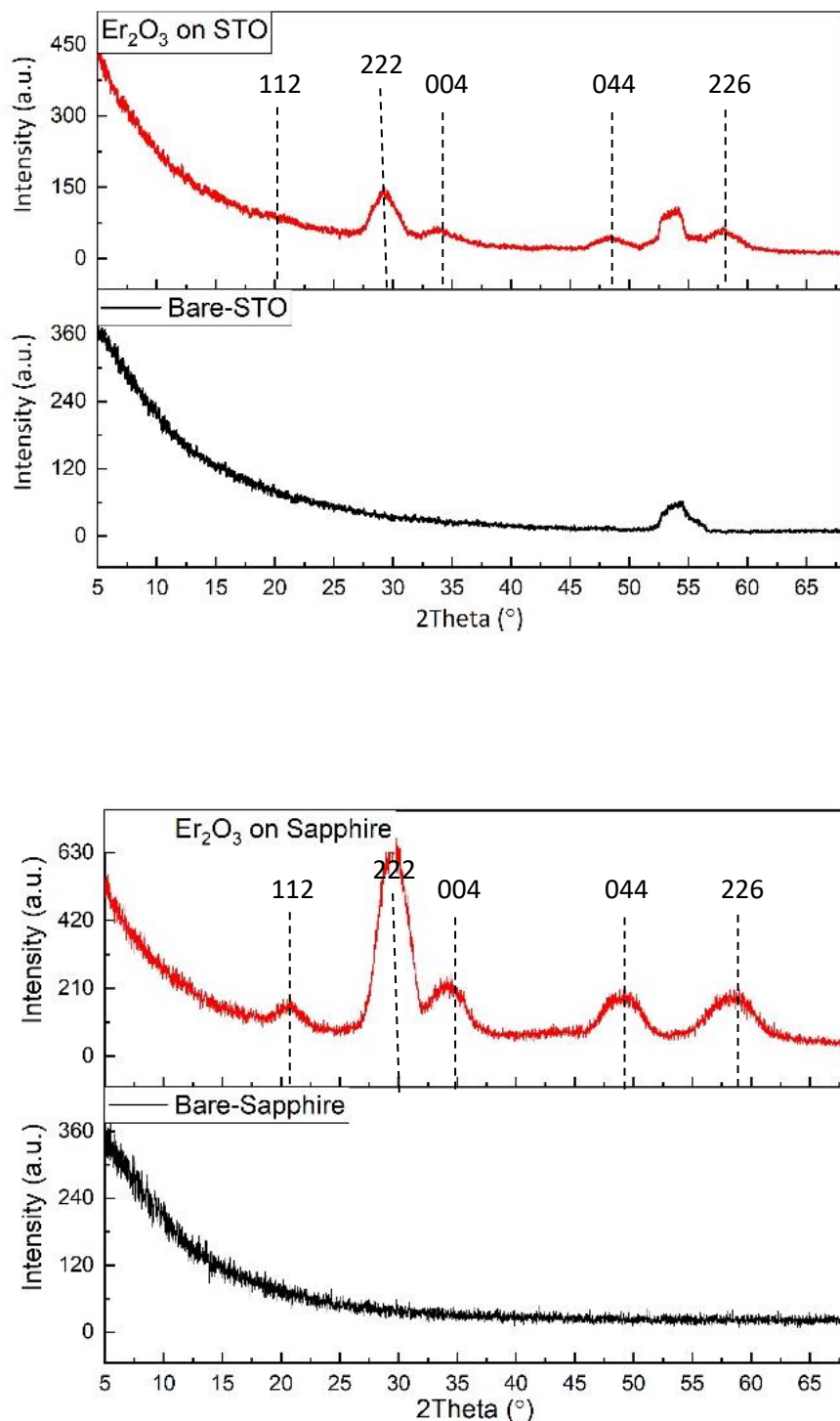
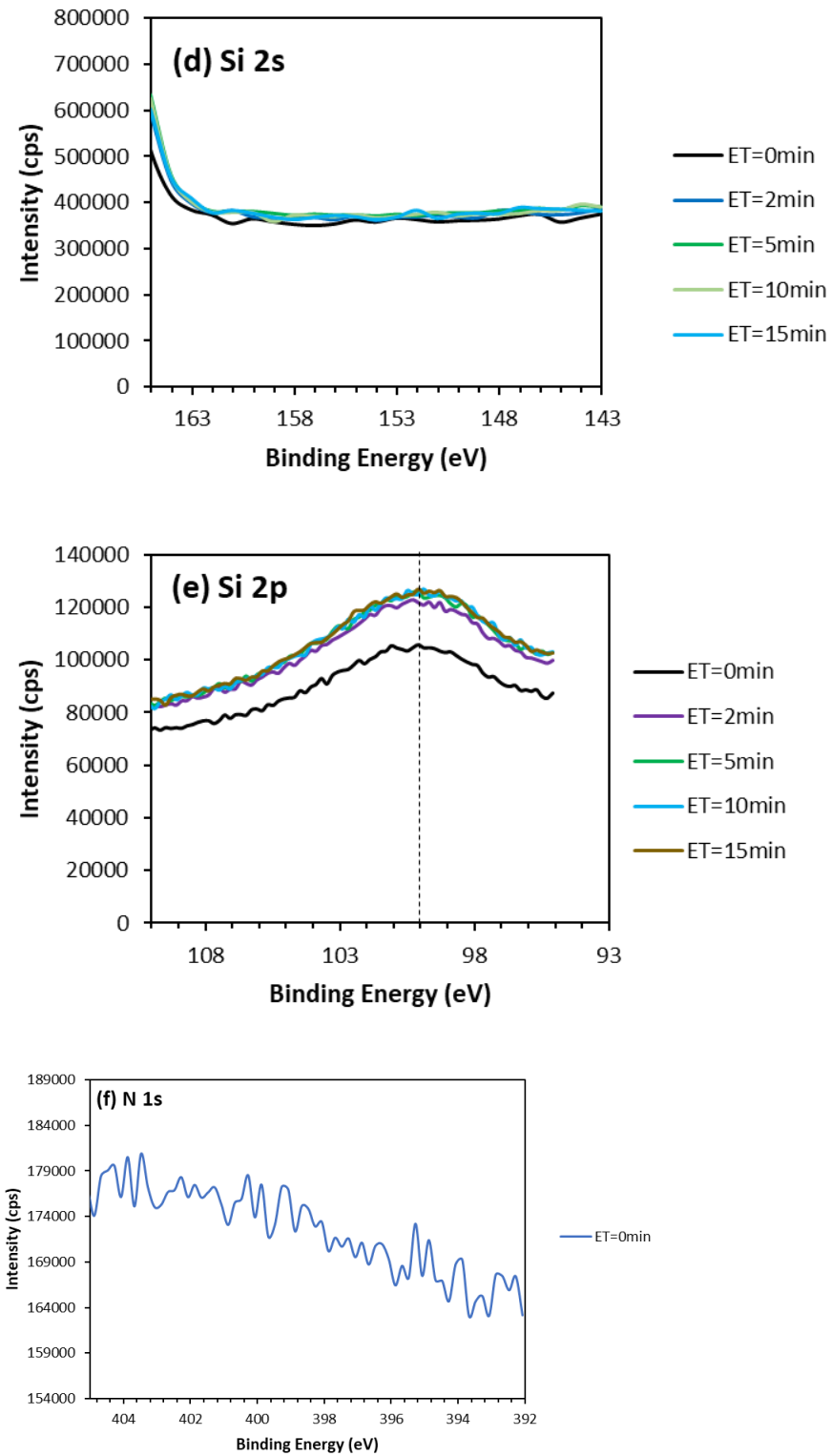


**Figure S9.** High-resolution XPS spectra of Si2s (d), Si2p (e), and N1s (f) ionization regions of a 35 nm thick  $\text{Er}_2\text{O}_3$  thin film grown on Si(100) at a substrate temperature of 200 °C with 1500 cycles. These plots are a continuation of Fig. 7 in the text, and are numbered (d)-(g) to be compatible with Fig. 7.



(g) C 1s

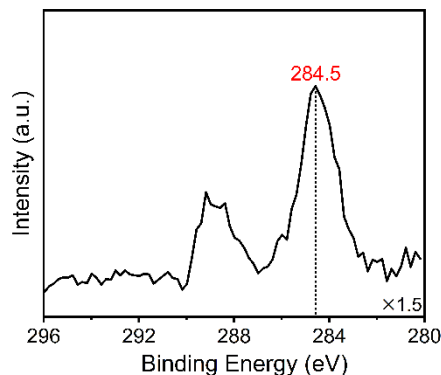


**Figure S10.** Er4d (a) and O1s (b) binding energy scans in the bulk of the film (after Ar ion sputtering), with peak fitting.

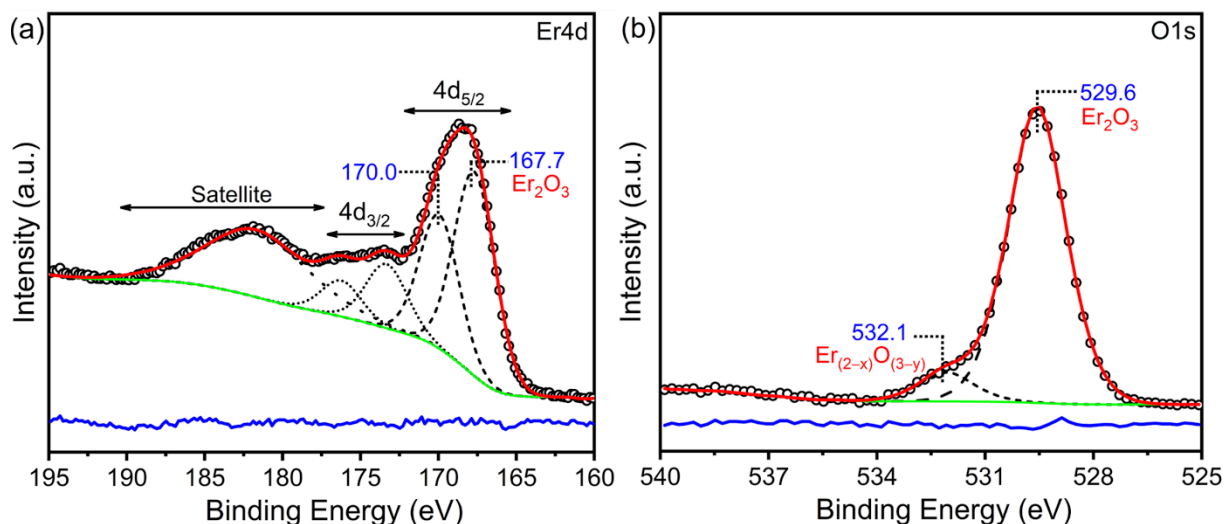


**Figure S11.** Overlapped EDS map of Er and Si elements. The numbered areas indicate the locations for the thickness measurements in Table S4.

